American Journal of Medical Genetics 125A:117–124 (2004)

Editor's Note

The papers by Bennett et al. and Gleeson et al. (next article, this issue) deal with the genetic basis and clinical classification of Joubert syndrome (JS) and related disorders. The authors of the first paper (below) took a functional gene and haplotype analysis approach and examined an "attractive" candidate gene for mutations in patients with JS. They mention that only one locus (9q34) for JS has been mapped thus far and that other families fail to map there, establishing genetic heterogeneity. Gleeson and colleagues extend work already published in this Journal that indicates that the molar tooth sign (MTS), previously felt to be specific for JS, can be seen as a component manifestation of a number of distinct conditions. It is now clear that JS belongs to a community of related disorders united by overlapping features including the MTS.

Also of significance to these papers, two groups independently mapped the phenotype of one (or more) of these "related disorders" to the pericentromeric region of chromosome 11. This work is published in the September issue of the American Journal of Human Genetics. I look forward to more advances in our understanding of this intriguing group of disorders.

John C. Carey
Editor

Joubert Syndrome: A Haplotype Segregation Strategy and Exclusion of the Zinc Finger Protein of Cerebellum 1 (*ZIC1*) Gene

Craig L. Bennett,* Melissa A. Parisi, Melissa L. Eckert, Huy M. Huynh, Phillip F. Chance, and Ian A. Glass

Division of Genetics and Development, Department of Pediatrics, University of Washington, School of Medicine, Seattle, Washington

Joubert syndrome (JS) is a rare autosomal recessive malformation syndrome, involving dysgenesis of the cerebellar vermis with accompanying brainstem malformations (comprising the molar tooth sign). JS is characterized by hypotonia, developmental delay, intermittent hyperpnea and apnea, and abnormal eye movements. A single locus for JS was previously identified on 9q34 in a consanguineous family of Arabian origin. However, linkage to this locus has subsequently been shown to be rare. We have ascertained 35 JS pedigrees for haplotype segregation analysis of genetic loci for genes with a putative role in cerebellar development. We examined the *ZIC1* gene as a functional candidate for JS as *Zic1*$^{-/-}$ null mice have a phenotype reminiscent of JS. We undertook mutational analysis of *ZIC1* by standard mutational analysis (dideoxy-fingerprinting (ddf)) of 47 JS probands, and fully sequenced the coding region in five of these probands. By these means, *ZIC1* was excluded from playing a causal role in most cases of JS as no disease-associated mutations were identified. Further, linkage to the *ZIC1* genetic locus (3q24) was excluded in 21 of 35 pedigrees by haplotype segregation analysis of closely spaced markers. The remaining 14 of 35 pedigrees were consistent with linkage. However, this number does not significantly depart from that expected by random chance (16.5) for this cohort. Therefore, this systematic approach has been validated as a means to prioritize functional candidate genes and enables us to confine mutational analysis to only those probands whose segregation is consistent with linkage to any given locus. © 2003 Wiley-Liss, Inc.

Grant sponsor: NIH (to P.F.C.); Grant number: NS38181.

*Correspondence to: Craig L. Bennett, Ph.D., Division of Genetics and Development, Department of Pediatrics, University of Washington, School of Medicine, Box 356320, 1959 NE Pacific Street, Seattle, WA 98195. E-mail: cbenet@u.washington.edu

Received 18 April 2003; Accepted 18 June 2003

DOI 10.1002/ajmg.a.20438

KEY WORDS: ***ZIC1*; cerebellum; linkage; Joubert syndrome; molar tooth sign**

INTRODUCTION

Joubert syndrome (JS) is a rare, autosomal recessive, neurological disorder, involving agenesis or dysgenesis of the cerebellar vermis with accompanying brainstem malformations. Diagnosis of JS is based upon a combination of specific clinical and brain imaging abnormalities. Clinical features, which are evident in early infancy, include hypotonia, episodic hyperpnea and apnea, abnormal eye movements, early developmental delay with subsequent mental retardation, and ataxia. Axial magnetic resonance imaging (MRI) of the upper brainstem shows a characteristic "molar tooth" appearance due to an abnormally deep interpeduncular fossa, prominent thickened superior cerebellar peduncles, and hypoplasia of the vermis [reviewed in: Maria et al., 1997; Chance et al., 1999]. Despite the delineation of apparently core features as diagnostic criteria for JS (hypotonia, ataxia, and molar tooth sign), the clinical nosology of syndromes having cerebellar vermis hypoplasia remains complex [Maria et al., 1999].

In the general population, JS may be present at ~1:100,000 to 1:150,000 (D. Flannery, personal communication). Saar et al. [1999] undertook homozygosity mapping in a consanguineous JS family of Arabian origin and identified linkage to chromosome 9q34. They investigated three other families of similar origin and demonstrated that only one other showed haplotypes consistent with linkage to the 9q34 locus, thereby establishing genetic heterogeneity for this entity. Moreover, we have suggested that linkage to the 9q34 JS locus is rare, as only one of eight multiplex JS pedigrees (3 consanguineous) were compatible with linkage at 9q34 [Blair et al., 2002; Bennett et al., 2003]. Several functional candidate genes have been identified based largely from insights gained by gene targeting or gene knock-out studies in mice.

Clearly, more JS loci are yet to be discovered, and towards this end we have undertaken a haplotype segregation analysis combined with a candidate gene approach. Thirty-five JS pedigrees were used to obtain haplotypes for four microsatellite markers encompassing the locus (3q24) for a strong functional JS candidate gene with a demonstrated role in cerebellar development (*ZIC1*). In cases where standard linkage analysis is difficult, yet significant numbers of informative pedigrees are available, specific loci within a heterogeneous disease can be uncovered utilizing a candidate gene approach [Beltran-Valero et al., 2002].

Many functional candidate genes for the JS have been suggested and several have been excluded [Blair et al., 2002]. One of the most attractive untested genes of this group is the *ZIC1* gene. In mouse, *Zic1* (zinc finger protein of cerebellum) expression is restricted to the nervous system, with highest levels observed in the cerebellum [Aruga et al., 1994]. *ZIC1* encodes a putative nuclear factor involved in early cerebellar differentiation, as well as in the maintenance of the phenotypic properties of the cerebellar granule cells [Aruga et al., 1994]. We therefore considered *ZIC1* a strong functional candidate for JS. By standard mutational methods, *ZIC1* was found non-causal in 47 JS probands. In addition, an approach characterized by haplotype segregation analysis has been demonstrated that will allow prioritization of functional candidate genes for future studies of JS.

MATERIALS AND METHODS

Subjects

The majority of patients were enrolled through a protocol of informed consent (University of Washington Human Subjects Division). Many families were ascertained through the JS Foundation (http://www.joubertsyndrome.org/). Medical histories and pedigrees were obtained by telephone interview and review of medical records, and by direct consultation at the Joubert Syndrome Foundation biennial meeting. Mutational analysis of the *ZIC1* gene was performed on 47 individuals who had clinical features consistent with Joubert syndrome. A diagnosis of JS was made according to published criteria including: hypotonia; ataxia; cerebellar vermis hypoplasia and associated "molar tooth sign" on MRI when available; developmental delay; episodic tachypnea and apnea; and abnormal eye movements [Saraiva and Baraitser, 1992; Steinlin et al., 1997; Maria et al., 1999]. Eighteen of the JS patients in this study have been previously described [Pellegrino et al., 1997].

Forty-four of the 47 JS probands (94%) had cerebellar vermis hypoplasia, which included documentation of the molar tooth sign in 57%. Breathing pattern abnormalities consisting of tachypnea and/or apnea in the newborn period were reported in 74%, and abnormal eye movements consisting of oculomotor apraxia and/or nystagmus were identified in 72%. Developmental delays were almost universal; present in 94% of the probands (for 3 patients, there was no information available regarding their development). Retinal changes were identified in 13%, while colobomas were seen in 11%. Renal abnormalities were identified in 21%, with cystic kidney disease or nephronophthisis diagnosed in 9%. Polydactyly was present in 15% of affected siblings. The incidence of colobomas and polydactyly in our cohort is greater than those previously described [Pellegrino et al., 1997] but similar to other reports [Saraiva and Baraitser, 1992]. Renal anomalies have been described in 21% of individuals in another series [Steinlin et al., 1997], although a great deal of variability in reports of retinal and renal changes have been noted [Maria et al., 1999].

Of the 47 probands, 22 were drawn from families included in haplotype analysis. The core diagnostic features of these 22 families included the following: 95% with cerebellar vermis hypoplasia and 73% with a reported molar tooth sign; 77% with respiratory abnormalities; 77% with abnormal eye movements; and 100% with developmental delays. Other clinical features included: 18% with retinal involvement, 5% with

coloboma, 18% with renal involvement, and 18% with polydactyly. The only notable difference within this subgroup in comparison with the 47 probands is the increased documentation of the molar tooth sign, which probably reflects improved imaging in many of the JS pedigrees more recently ascertained, as opposed to singleton individuals included in mutational analysis who were ascertained prior to characterization of the molar tooth sign in 1997 [Maria et al., 1997].

Microsatellite Analysis

Peripheral blood lymphocytes were harvested from patient blood and genomic DNA was isolated using standard methods [Chance et al., 1998]. Polymorphic markers used in this study (Fig. 1) were from the Généthon human genetic linkage map [Dib et al., 1996]. PCR reactions for linkage analysis were set up in a total volume of 5.5 μl: 50 mM KCl, 10 mM Tris-HCl (pH 8.3),

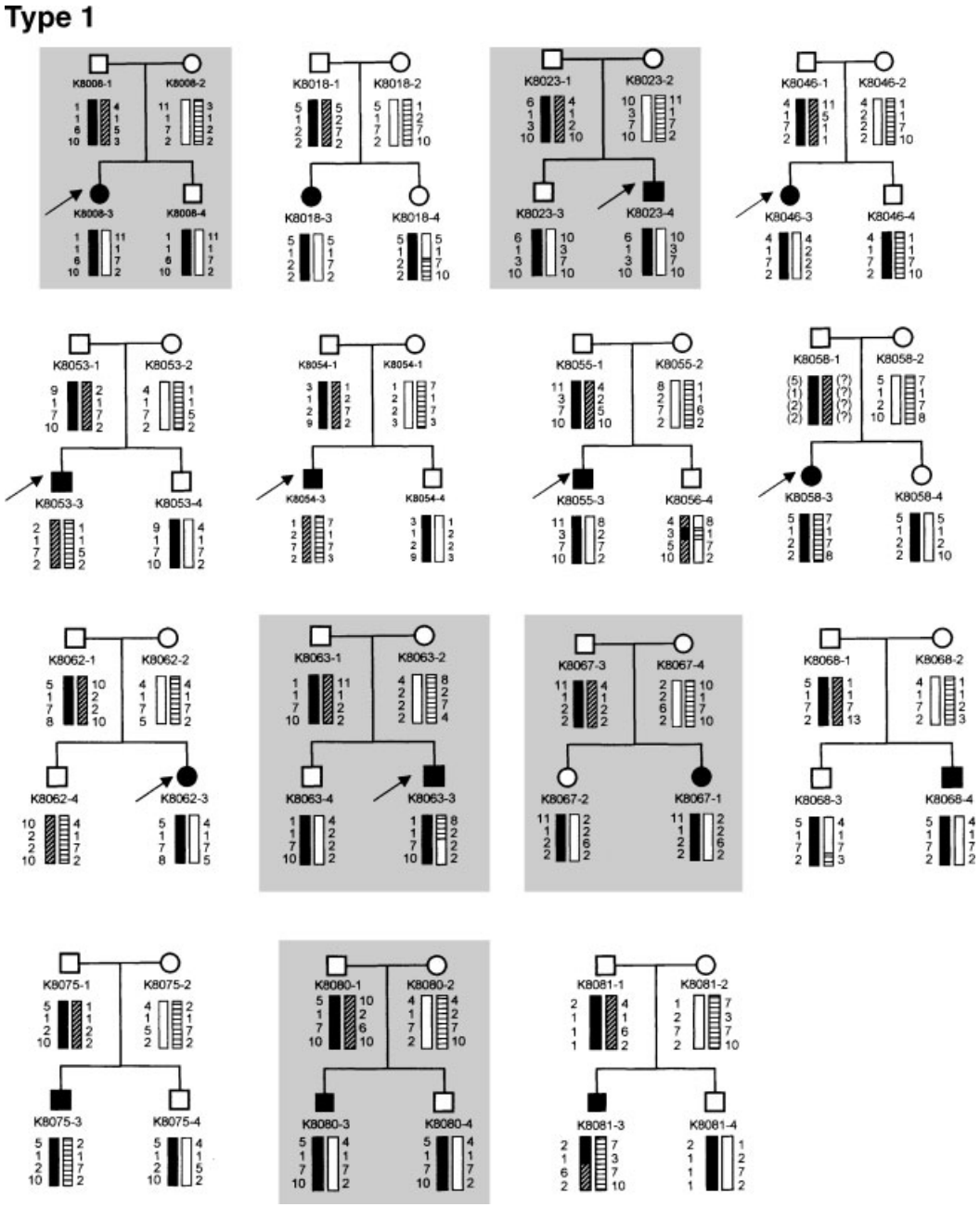

Fig. 1. Pedigrees have been categorized based on their linkage power, from Type 1 the lowest, to Type 9 the highest. Where pedigrees are shaded, linkage can be excluded based on the criteria described in the "Materials and Methods." Where parental haplotypes have been inferred, alleles are in parenthesis. In pedigree K8003, two siblings demonstrated mis-inheritance (*). We believe that this apparent mis-inheritance may have arisen from a natural expansion of allele 2 to 3 of the paternal 11-1-6-2 haplotype. Pedigrees from which probands were tested by dideoxy-fingerprinting (ddF) are indicated (→).

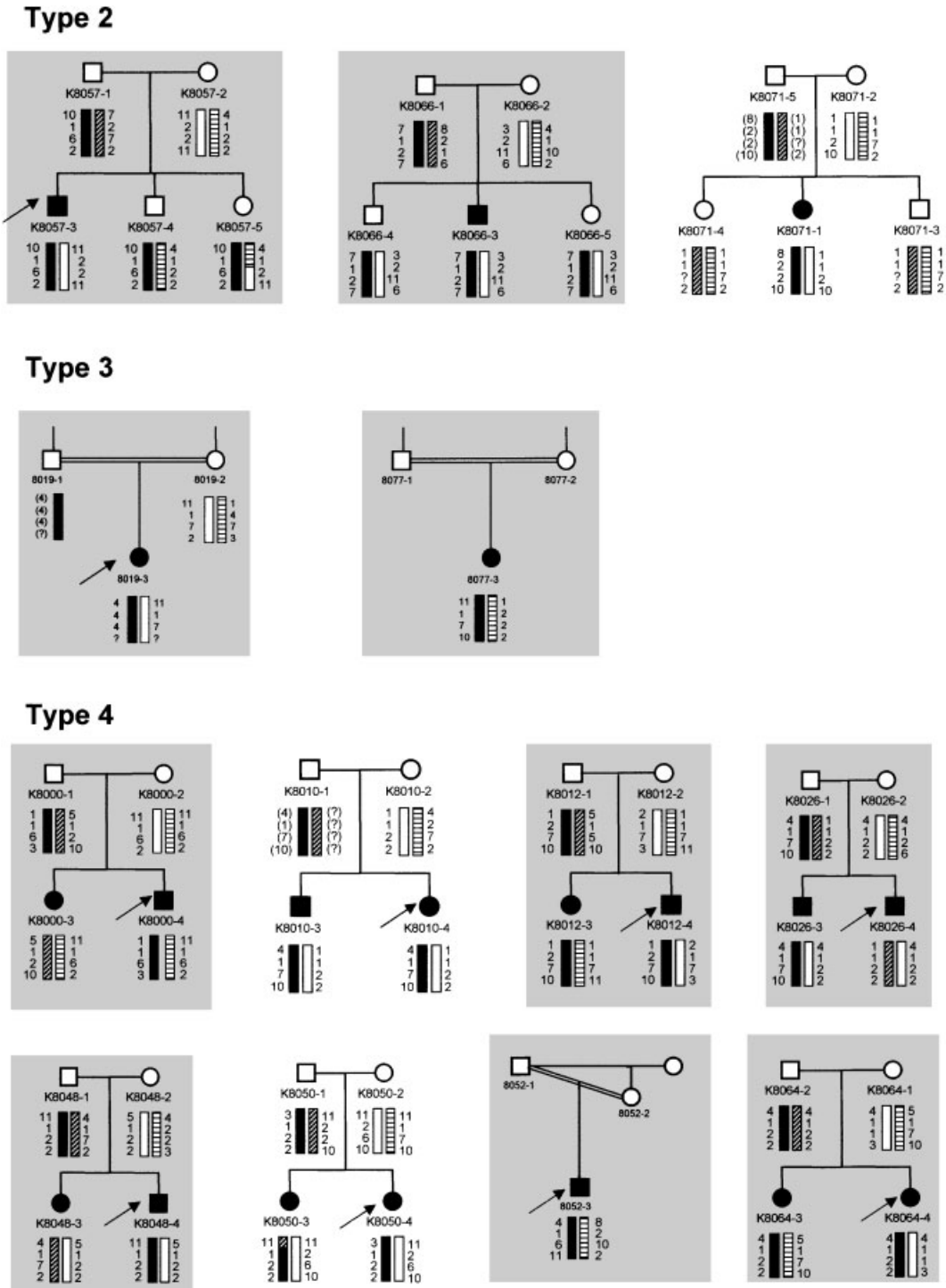

Fig. 1. (*Continued*)

2.5 mM $MgCl_2$, 330 μM each NTP, 2 pMole sense and antisense primers, 5% dimethyl sulfoxide (DMSO), 0.2 U HotMaster Taq polymerase (Eppendorf, Westbury, NY), and 50 ng of DNA template. PCR amplification was performed on a MJ PTC-100 thermal cycler with initial denaturation at 94°C for 2 min, followed by 35 cycles of 94°C for 20 s, 55°C for 20 s, 65°C for 90 s, a final extension at 72°C for 10 min and hold at 4°C. PCR amplicons were detected using 6-FAM (6-carboxy-fluorescein) fluorescence sense primers obtained from Applied Biosystems (Foster City, CA). PCR reactions were diluted 1:15 to 1:32 in water and 1–5 μl of this dilution was added to 12 μl of GeneScan cocktail (1 ml de-ionized formamide [Sigma-Aldrich Corp., St. Louis, MO] and 50 μl ROX

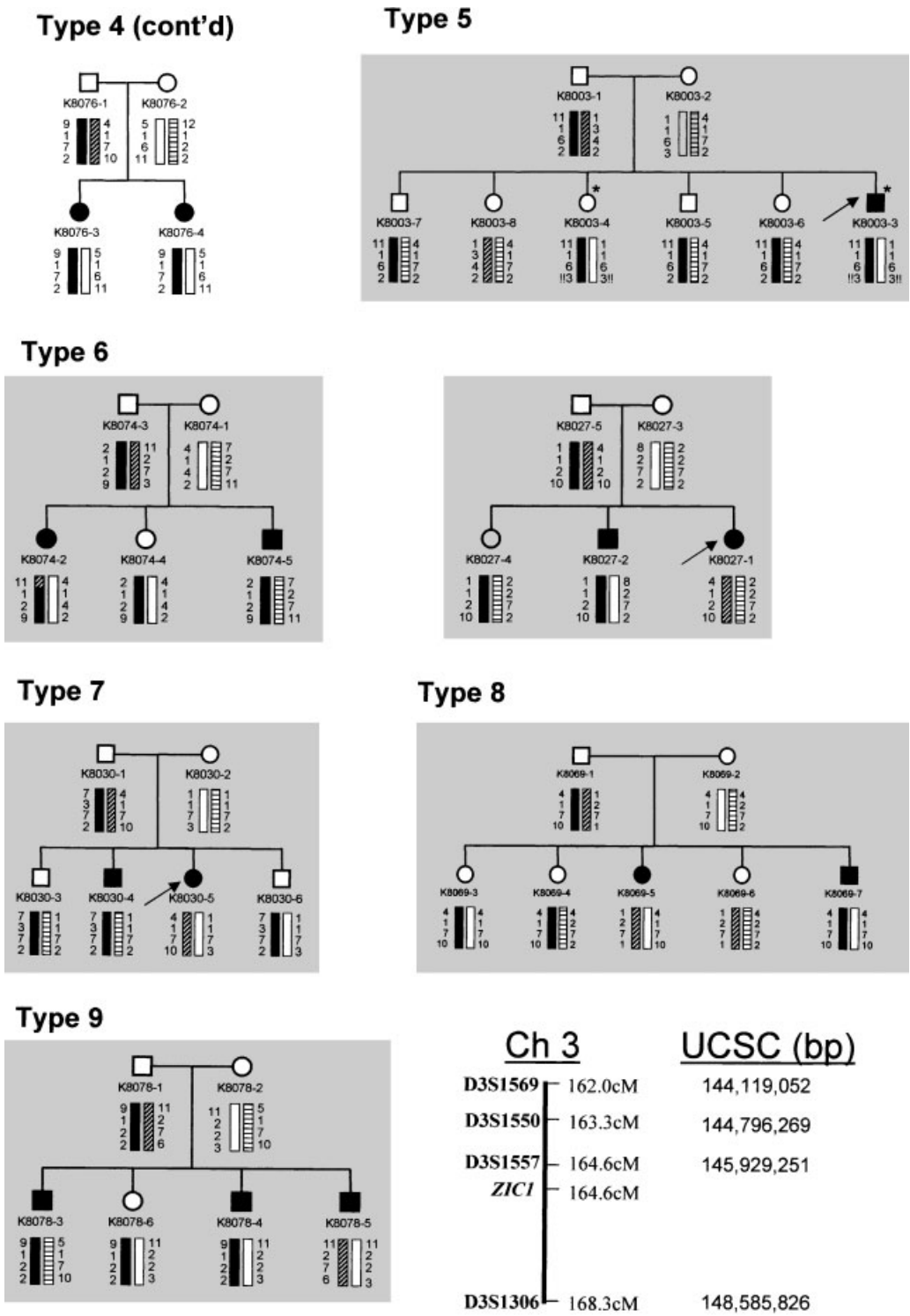

Fig. 1. (*Continued*)

400HD size standard). Following capillary electrophoresis of the PCR products for 24 min with a 10 s injection time for each sample using the Performance Optimized Polymer 4 (POP-4) (PE Biosystems, Foster City, CA), the results were analyzed using GeneScan® v. 2.5.2 software (Applied Biosystems). Genotypes were scored and haplotypes constructed using CYRILLIC™ (version 2.1). Marker allele sizes and frequencies were obtained from the Genome Data Base (GDB) or determined from our dataset if discrepancies were present.

ddF Mutation Analysis and Direct Sequencing

The genomic structure of *ZIC1* was determined by BLAST search of the human genomic sequence database with *ZIC1* cDNA sequence (NM_003412). A genomic BAC clone 649A16 (AC092959) was identified which included the entire *ZIC1* gene. Primers were designed from flanking genomic sequence for amplification of six *ZIC1* amplicons from patient genomic DNA to encompass the 1,344 bp of coding sequence and at least 50 bp of each intron/exon boundary. Primer sequences and amplification conditions are available from the authors on request. Mutation analysis of amplicons was carried out via dideoxy-fingerprinting (ddF) following cycle sequencing using standard methods [Liu and Sommer, 1994]. PCR amplified products were purified and cycle sequenced (Sequitherm Excell II DNA sequencing kit, Epicenter Technologies, Madison, WI) using a single termination mix. In brief, the technique of ddF is a combination of dideoxy termination DNA sequencing and single-strand conformation polymorphism (SSCP) analysis. ddF is performed by electrophoresing one labeled dideoxy termination reaction through a non-denaturing gel and the resulting pattern can be divided into a "dideoxy component" and an "SSCP component." If dideoxy CTP (ddCTP) is utilized for the termination reaction, the dideoxy component is abnormal when an extra segment is produced by a sequence change that creates an extra C or when a segment is eliminated by a change of C to another base. The SSCP component is informative if abnormal mobility is detected in one or more of the segments. As the gel is non-denaturing, all fragments subsequent to a conformational change are shifted; essentially amplifying what is normally seen in SSCP.

Forty-eight sample reactions were loaded onto 0.5× MDE gel (FMC) and separated by electrophoresis for 4.5 hr at 12 W with fan cooling. A PCR amplification product containing a known G→A polymorphism was included as control. Termination products were visualized on X-ray sensitive film (X-OMAT AR, Kodak) after 1–3 day exposure.

Direct sequence analysis was performed on PCR amplified fragments using the ABI PRISM Big Dye Terminator Cycle Sequencing Ready Reaction Kit (Perkin-Elmer, Foster City, CA), and chromatograms were generated on an Applied Biosystems High Through-Put Capillary Electrophoresis sequencer.

Haplotype Segregation Analysis

Our approach was to determine whether *ZIC1* haplotypes were either consistent with linkage to the *ZIC1* locus or excluded linkage to the *ZIC1* locus, for the 35 JS pedigrees in which parental and sibling DNA was available. If chromosome 3q24 haplotypes indicated that one of two or more affected siblings had inherited at least one different parental chromosome, linkage was excluded. If one affected and one or more unaffected siblings inherited the same parental chromosomes, linkage was also excluded.

To determine what proportion of the 35 pedigrees would appear consistent with linkage by chance for each haplotype, we first ranked the pedigrees into nine types (1 through 9 in increasing order of statistical power). We then determined by probability (1/log of Max LOD score possible), the frequency that each pedigree-type would appear linked by random chance (Table I). Taken together, these estimates suggest that on average, 16.5 of the 35 JS pedigrees would be consistent with linkage to a given locus by random chance (Table I). Clearly, this will be made up predominantly from the least informative pedigrees with two siblings, of which only one is affected (Type 1).

Two-point LOD scores were calculated between polymorphic markers and the *ZIC1* locus (3q24), by means of the computer program LINKAGE (version 5.1) [Lathrop et al., 1985]. LOD scores (Z) were calculated under a model of recessive inheritance. Penetrance was taken as 0.99 for homozygous affected individuals. The frequency of the mutant allele was assumed to be 0.0001 (1:10,000). Genetic distances for microsatellite markers were taken from Généthon: D3S1569; D3S1550; D3S1557 and D3S1306 (162.0, 163.3, 164.6, and 168.3 cM, respectively) (Fig. 1).

RESULTS

Mutational Analysis of the *ZIC1* Gene

All coding exons of *ZIC1* including at least 50 bp of intron/exon boundary were screened for mutations in the genomic DNA of 47 unrelated JS patients, and no mutations were identified. The coding sequence of *ZIC1* is 1,344 bp and consists of three exons on BAC clone 649A16. The largest exon at 1,011 bp was amplified as three overlapping fragments, so that the entire coding

TABLE I. Probability That Each JS Pedigree Type Will Appear Linked at Any Given Locus

Pedigree type	No. of pedigrees	No. of affected sibs	No. of unaffected sibs	Probability of linkage by chance (P=)
Type 1	15	1	1	0.750
Type 2	3	1	2	0.563
Type 3	2 (1st cousin mating)	1	0	0.316
Type 4	8	2	0	0.250
Type 4	1 (Father/daughter mating)	1	0	0.250
Type 5	1	1	5	0.240
Type 6	2	2	1	0.188
Type 7	1	2	2	0.140
Type 8	1	2	3	0.105
Type 9	1	3	1	0.047

16.5 of the 35 JS pedigrees are expected to be consistent with linkage to a given locus by random chance: $[(15 \times 0.75) + (3 \times 0.563) + (2 \times 0.316) + (8 \times 0.250) + (1 \times 0.250) + (2 \times 0.240) + (1 \times 0.188) + (1 \times 0.140) + (1 \times 0.105) + (1 \times 0.047) = 16.5]$.

sequence could be amplified as six PCR fragments. Proband DNA from five pedigrees was sequenced as well as any samples that gave spurious bands by ddF analysis. No disease-associated mutations were detected either by ddF or DNA sequencing analysis. We did observe an 186A → G transition from the published *ZIC1* cDNA sequence (NM_003412) in all samples tested, including normal controls.

Genetic Haplotype Analysis

Analysis of the 35 JS pedigrees (Fig. 1) was performed using four microsatellite markers, D3S1569, D3S1550, D3S1557, and D3S1306. These markers cover a 6 cM interval on chromosome 3, flanking the *ZIC1* gene at chromosome 3q24. Of the 35 pedigrees, 14 could not exclude linkage to the *ZIC1* 3q24 loci. A chi-squared test result of $P > 0.5$ (at one df), clearly shows that the number of observed JS pedigrees consistent with linkage (14, observed) is not significantly different from the number expected by chance (16.5, expected).

LOD scores determined for the three most informative JS pedigrees (K8030, K8069, and K8078), are shown in Table II. Linkage could be excluded to 1–5 cM in pedigree K8030 with marker D3S1557. Linkage could be excluded to 5–10 cM in pedigree K8078 with markers D3S1569 and D3S1557. Using the SimWalk2 program (version 2.83), performing non-parametric linkage analysis, we estimated a potential maximum LOD score of 1.3 could be obtained with pedigree K8078, the most informative family. This LOD score of 1.3 is equivalent to the probability of $P = 0.047$ calculated for this Type 9 pedigree.

DISCUSSION

The Joubert Syndrome (JS) remains a complex developmental disorder with few clues to the underlying molecular mechanism. Given the difficulty in identifying the major genetic loci for JS by standard genetic approaches [Saar et al., 1999; Blair et al., 2002; Bennett et al., 2003], we are taking a combined haplotype segregation analysis and functional candidate gene approach to prioritize candidate genes. The 35 JS pedigrees will be used to obtain haplotypes at the loci of JS candidate genes with a demonstrated role in cerebellar development, which can then be prioritized for mutational screening. For this study we undertook the mutational screening of *ZIC1* concomitantly with the haplotype analysis of the *ZIC1* genetic locus at 3q24.

A similar approach to what we have attempted has recently been used with success to identify a gene for the Walker-Warburg syndrome (WWS) (OMIM: 23667). WWS has a phenotype similar to muscle-eye-brain disease (MEB) and Fukuyama congenital muscular dystrophy (FCMD) (OMIM: 25380). While the genes for MEB and FCMD had previously been cloned, genetic loci for WWS remained elusive. A genome-wide linkage analysis was performed in ten consanguineous families with WWS [Beltran-Valero et al., 2002], and no potential loci could be confirmed using either a one or two loci premise. The authors adopted a candidate-gene approach in combination with homozygosity mapping in 15 consanguineous WWS families. Candidate genes were selected based on the known roles of the FCMD and MEB genes and hypothesized *O*-mannosyl glycan synthesis involvement in WWS. Analysis of the locus for *O*-mannosyltransferase 1 (*POMT1*), revealed homozygosity in 5 of the 15 families, and subsequent sequencing of the *POMT1* gene revealed mutations in 6 of the 30 families with WWS [Beltran-Valero et al., 2002].

In an attempt to further understand the role ZIC1 may play in cerebellar development, Aruga et al. [1998] generated homozygous *Zic1* knockout mice ($Zic1^{-/-}$). During postnatal development, the $Zic1^{-/-}$ mice are markedly ataxic and their cerebella are hypoplastic. The foliation pattern is abnormal, and the anterior part of the cerebellar vermis is most severely affected [Aruga et al., 1998]. Mortality is high in $Zic1^{-/-}$ mice, as most die within the first postnatal month. *Zic1* heterozygotes ($Zic1^{+/-}$) demonstrate significant abnormalities in locomotor tests, including hanging, spontaneous locomotor activity, and stationary testing [Ogura et al., 2001]. Interestingly, while $Zic1^{-/-}$ mice result in cerebellar malformations with severe ataxia, *Zic2* null mutants

TABLE II. LOD Scores at Various Recombination Fractions for Markers on Chromosome-3, in Three JS Pedigrees

Marker	0.0	0.01	0.05	0.10	0.20	0.30	0.40
K8030							
D3S1569	−infini	−1.36	−0.68	−0.41	−0.18	−0.07	−0.02
D3S1550	−infini	−1.36	−0.68	−0.41	−0.18	−0.07	−0.02
D3S1557	−infini	−2.85	−1.48	−0.91	−0.39	−0.15	−0.04
D3S1306	0.00	0.00	0.00	0.00	0.00	0.00	0.00
K8069							
D3S1569	−infini	−1.45	−0.76	−0.48	−0.21	−0.08	−0.02
D3S1550	−infini	−1.32	−0.62	−0.34	−0.11	−0.03	−0.00
D3S1557	−infini	−1.04	−0.39	−0.16	−0.01	0.01	0.01
D3S1306	0.00	0.00	0.00	0.00	0.00	0.00	0.00
K8078							
D3S1569	−infini	−4.09	−2.06	−1.25	−0.53	−0.20	−0.05
D3S1550	−infini	−2.96	−1.55	−0.95	−0.41	−0.16	−0.04
D3S1557	−infini	−4.09	−2.06	−1.25	−0.53	−0.20	−0.05
D3S1306	0.12	0.12	0.09	0.06	0.02	0.00	0.00

develop holoprosencephaly and spina bifida. It has recently been shown that the *Zic1* and *Zic2* genes have a coordinated role in cerebellar development, as either $Zic1^{+/-}$ heterozygotes or Zic2 heterozygous knockdown mice ($Zic2^{+/kd}$) have a cerebellum almost indistinguishable from wildtype. However, $Zic1^{+/-}Zic2^{+/kd}$ compound heterozygotes develop a clearly abnormal cerebellar structure [Aruga et al., 2002]. Despite the different inheritance pattern from the autosomal recessive human condition of JS, $Zic1^{+/-}$ heterozygous mice exhibit an abnormal locomotor phenotype that is reminiscent of deficits seen in patients with JS. Comparisons of the neuropathy seen in the brains of $Zic1^{-/-}$ mice and human with JS are problematic largely because of the limited human post-mortem samples available and the variability of the findings [Friede and Boltshauser, 1978; Yachnis and Rorke, 1999]. Both $Zic1^{-/-}$ mice and JS patients have involvement of the midline vermal structures. However, one contrast is clear; the cerebellar hemispheres are not as severely affected in the JS malformation process from the neuropathology and the MRI evaluations available at this point [Yachnis and Rorke, 1999], whereas those in $Zic1^{-/-}$ mice are hypoplastic in both structures of the cerebellum [Aruga et al., 1998]. A contrast that may be present is that human neuropathology demonstrates brainstem abnormalities [Friede and Boltshauser, 1978; Yachnis and Rorke, 1999] whereas this has not been described in $Zic1^{-/-}$ mice.

We screened the *ZIC1* gene by standard mutational analysis in 47 probands and found no disease-associated mutations. Further, we also sequenced the complete *ZIC1* coding region from five JS probands and detected no causative mutations. We believe that given the large cohort of JS pedigrees screened and the fact that observed linkage to the 3q24 locus was not greater than what is expected by chance, *ZIC1* can be effectively excluded from playing a functional role in most cases of JS. Contiguously, we have put into place an effective means to analyze the loci of many JS candidate genes, including those within the candidate interval of the only known locus on chromosome 9q34, which should prove an invaluable resource for finding the causative gene(s). The most promising untested JS candidate genes may include: (1) Astrotactin (*ASTN*); Atonal Drosophila Homolog of 1; ATOH1 (*MATH1*); Paired Box Gene 2 (*PAX2*) and Paired Box Gene 5 (*PAX5*). These candidate genes encode proteins that are thought to play roles in cellular functions such as neuronal adhesion, transcription factors involved in nervous system development and other protein regulators of complex steps of early CNS development. The loci encompassing these JS candidate genes will be immediately amenable to testing via the methods we have outlined here.

ACKNOWLEDGMENTS

We thank patients and their families for participation. We also thank the Joubert Syndrome Foundation for its contribution to this study. We thank Karen Barnett M.S. for assistance in contacting JS families and Richard Peet for growing and maintaining patient cell lines.

REFERENCES

Aruga J, Yokota N, Hashimoto M, Furuichi T, Fukuda M, Mikoshiba K. 1994. A novel zinc finger protein, zic, is involved in neurogenesis, especially in the cell lineage of cerebellar granule cells. J Neurochem 63: 1880–1890.

Aruga J, Minowa O, Yaginuma H, Kuno J, Nagai T, Noda T, Mikoshiba K. 1998. Mouse Zic1 is involved in cerebellar development. J Neurosci 18: 284–293.

Aruga J, Inoue T, Hoshino J, Mikoshiba K. 2002. Zic2 controls cerebellar development in cooperation with zic1. J Neurosci 22:218–225.

Beltran-Valero de, Bernabe D, Currier S, Steinbrecher A, Celli J, Van Beusekom E, Van Der Zwaag B, Kayserili H, Merlini L, Chitayat D, Dobyns WB, Cormand B, Lehesjoki AE, Cruces J, Voit T, Walsh CA, Van Bokhoven H, Brunner HG. 2002. Mutations in the *O*-mannosyltransferase gene *POMT1* give rise to the severe neuronal migration disorder Walker-Warburg syndrome. Am J Hum Genet 71:1033–1043.

Bennett CL, Meuleman J, Chance PF, Glass IA. 2003. Clinical and genetic aspects of the Joubert syndrome: A disorder characterised by cerebellar vermian hypoplasia and accompanying brainstem malformations. Current Genomics 4:123–129.

Blair IP, Gibson RR, Bennett CL, Chance PF. 2002. A search for genes involved in Joubert syndrome: Evidence that one or more major loci are yet to be identified and exclusion of candidate genes *EN1*, *EN2*, *FGF8*, and *BARHL1*. Am J Med Genet 107:190–196.

Chance PF, Rabin BA, Ryan SG, Ding Y, Scavina M, Crain B, Griffin JW, Cornblath DR. 1998. Linkage of the gene for an autosomal dominant form of juvenile amyotrophic lateral sclerosis to chromosome 9q34. Am J Hum Genet 62:633–640.

Chance PF, Cavalier L, Satran D, Pellegrino JE, Koenig M, Dobyns WB. 1999. Clinical nosologic and genetic aspects of Joubert and related syndromes. J Child Neurol 14:660–666; Discussion 669–672.

Dib C, Faure S, Fizames C, Samson D, Drouot N, Vignal A, Millasseau P, Marc S, Hazan J, Seboun E, Lathrop M, Gyapay G, Morissette J, Weissenbach J. 1996. A comprehensive genetic map of the human genome based on 5,264 microsatellites. Nature 380:152–154.

Friede R, Boltshauser E. 1978. Uncommon syndromes of cerebellar vermis aplasia. I Joubert syndrome. Dev Med Child Neurol 20:758–763.

Lathrop GM, Lalouel JM, Julier C, Ott J. 1985. Multilocus linkage analysis in humans: Detection of linkage and estimation of recombination. Am J Hum Genet 37:482–498.

Liu Q, Sommer SS. 1994. Parameters affecting the sensitivities of dideoxy fingerprinting and SSCP. PCR Methods Appl 4:97–108.

Maria BL, Hoang KB, Tusa RJ, Mancuso AA, Hamed LM, Quisling RG, Hove MT, Fennell EB, Booth-Jones M, Ringdahl DM, Yachnis AT, Creel G, Frerking B. 1997. "Joubert syndrome" revisited: Key ocular motor signs with magnetic resonance imaging correlation. J Child Neurol 12:423–430.

Maria BL, Boltshauser E, Palmer SC, Tran TX. 1999. Clinical features and revised diagnostic criteria in Joubert syndrome. J Child Neurol 14:583–590; Discussion 590–591.

Ogura H, Aruga J, Mikoshiba K. 2001. Behavioral abnormalities of Zic1 and Zic2 mutant mice: Implications as models for human neurological disorders. Behav Genet 31:317–324.

Pellegrino JE, Lensch MW, Muenke M, Chance PF. 1997. Clinical and molecular analysis in Joubert syndrome. Am J Med Genet 72:59–62.

Saar K, Al-Gazali L, Sztriha L, Rueschendorf F, Nur EKM, Reis A, Bayoumi R. 1999. Homozygosity mapping in families with Joubert syndrome identifies a locus on chromosome 9q34.3 and evidence for genetic heterogeneity. Am J Hum Genet 65:1666–1671.

Saraiva JM, Baraitser M. 1992. Joubert syndrome: A review. Am J Med Genet 43:726–731.

Steinlin M, Schmid M, Landau K, Boltshauser E. 1997. Follow-up in children with Joubert syndrome. Neuropediatr 28:204–211.

Yachnis AT, Rorke LB. 1999. Neuropathology of Joubert syndrome. J Child Neurol 14:655–659; Discussion 669–672.